

- Christakos, J. I. Morgan, E. Mugnaini, unpublished observations.
15. R. J. Mullen, *Society for Neuroscience Symposia* (Society for Neuroscience, Bethesda, MD, 1977), vol. 2, pp. 47–65; K. Herrup and R. J. Mullen, *Dev. Brain Res.* **1**, 475 (1981); D. Goldowitz, *Neuron* **2**, 1565 (1989).
16. J. Rossant, M. Vjih, L. D. Siracusa, V. M. Chapman, *J. Embryol. Exp. Morphol.* **73**, 179 (1983); L. D. Siracusa *et al.*, *ibid.*, p. 163.
17. N. Feder, *Nature* **263**, 67 (1976); K. Herrup and R. J. Mullen, *J. Cell Science* **40**, 21 (1979); R. J. Smeyne and D. Goldowitz, *Dev. Brain Res.*, in press; K. Herrup and R. J. Mullen, *ibid.* **1**, 475 (1981).
18. K. Schilling, R. J. Smeyne, J. Oberdick, J. I. Morgan, unpublished observation.
19. We thank T. Curran and C. Stewart for critical reading of the manuscript and our long-time collaborator, E. Mugnaini, for valuable advice. Partially supported by National Research Service Award 1 F32 NS 08680-01 (to R.J.S.).

21 November 1989; accepted 6 February 1990

## Unusual Topogenic Sequence Directs Prion Protein Biogenesis

CHARLES D. LOPEZ, C. SPENCER YOST, STANLEY B. PRUSINER, RICHARD M. MYERS, VISHWANATH R. LINGAPPA

**Biosynthetic studies of the prion protein (PrP) have shown that two forms of different topology can be generated from the same pool of nascent chains in cell-free translation systems supplemented with microsomal membranes. A transmembrane form is the predominant product generated in wheat germ (WG) extracts, whereas a completely translocated (secretory) form is the major product synthesized in rabbit reticulocyte lysates (RRL). An unusual topogenic sequence within PrP is now shown to direct this system-dependent difference. The actions of this topogenic sequence were independent of on-going translation and could be conferred to heterologous proteins by the engineering of a discrete set of codons. System-dependent topology conferred by addition of RRL to WG translation products suggests that this sequence interacts with one or more cytosolic factors.**

**S**ECRETORY AND TRANSMEMBRANE proteins acquire their orientation with respect to the membrane of the endoplasmic reticulum (ER) in a manner that is usually both predictable and absolute (1). This reflects the action of discrete regions within such nascent proteins, termed signal and stop-transfer sequences, that initiate and terminate translocation across the ER (2). Studies in eukaryotic cell-free systems have revealed that at least some topogenic sequence actions are mediated by receptor proteins (3–6). The subcellular components that function in such systems appear conserved. Thus, mRNA from any tissue or species can be translated in cytosolic extracts of either WG or RRL (7, 8). When these translation systems are supplemented with microsomal membranes derived from the ER, the newly synthesized protein achieves a topology identical to that

observed in the ER in vivo (9). Topology can be assayed by means of proteases to distinguish domains protected by the lipid bilayer (10, 11).

An exception to this conservation of components occurs during biogenesis of the prion protein (PrP). PrP, a brain glycoprotein, exists in two isoforms: (i) PrP<sup>C</sup>, which is found in normal brain and is expressed at specific times during development (12, 13), and (ii) PrP<sup>Sc</sup>, which is a component of the infectious agent causing scrapie (a degenerative neurologic disease of animals that is related to several diseases of humans) (14). The primary amino acid sequences of PrP<sup>C</sup> and PrP<sup>Sc</sup> are identical (14, 15). Both isoforms contain a phosphatidylinositol glycolipid anchor at their COOH-terminals that is cleavable by a phosphatidylinositol-specific phospholipase C (PIPLC) (16). However, only PrP<sup>C</sup> is released from cells when treated with PIPLC (17). These findings are consistent with a difference between the two isoforms in either subcellular localization or transmembrane orientation.

Likewise, PrP synthesized in vitro displays two system-dependent topologies. When a cloned cDNA encoding PrP is expressed by transcription-linked translation in WG, a transmembrane form predominates (18). When the same transcript is translated in RRL, the predominant prod-

uct is a completely translocated (that is, secretory) protein (19). Some feature or process occurring in the cytosolic fraction seems to recognize information within nascent PrP to direct transmembrane or secretory forms.

The characteristic transmembrane form of PrP observed in WG spans the bilayer twice, such that both the NH<sub>2</sub>- and COOH-terminal domains are within the lumen of the ER (Fig. 1A) (18). The first membrane-spanning domain synthesized, TM1, is approximately 90 amino acid residues from the NH<sub>2</sub>-terminal-cleaved signal sequence. Therefore it seemed plausible that the difference in PrP topology observed in WG versus RRL was a reflection of a difference in the ability of these systems to stop translocation of the chain at TM1. One explanation for this difference might be that the rate of chain elongation (and hence the rate of chain translocation) is unequal in WG versus RRL, thereby influencing the extent of stop transfer at TM1.

Thus, the first step toward analysis of the molecular basis for the alternate fates in PrP biogenesis was to uncouple translocation of the chain from protein synthesis. Normally, translocation occurs only while peptide chains are in the process of being synthesized (co-translationally). By truncation of a cDNA within the coding region, it becomes possible to generate mRNA lacking a termination codon. In this case, the initial engaged ribosome will be unable to release the nascent peptide chain. These nascent chains remain translocation-competent even in the absence of further chain elongation (20).

PrP cDNA was truncated at a Hinc II site 74 codons 5' to the termination codon. Transcription-linked translation of this DNA (PrP/HcII) in either WG (Fig. 2) or RRL (Fig. 3) in the absence of microsomal membranes resulted in a nascent chain-ribosome complex in which PrP had been synthesized from the NH<sub>2</sub>-terminal through TM1. The translation product was presented to the membrane either co-translationally (with membranes present during its synthesis) or posttranslationally (with membranes added after completion of synthesis and in the presence of translation inhibitors). As expected for translocation-competent chains, cleavage of the signal sequence occurred in the presence of membranes either co- or post-translationally in both WG and RRL (Figs. 2 and 3). Unlike native PrP (18, 19), these truncated products were not glycosylated, since the recipient asparagine residues for N-linked carbohydrates were lost after truncation. Glycosylation has no influence on generation of either form of PrP, as shown by use of a tripeptide inhibitor of N-linked glycosylation in both WG and RRL (21).

C. D. Lopez, Department of Physiology, University of California, San Francisco, San Francisco, CA 94143.

C. S. Yost, Departments of Physiology and Anesthesia, University of California, San Francisco, San Francisco, CA 94143.

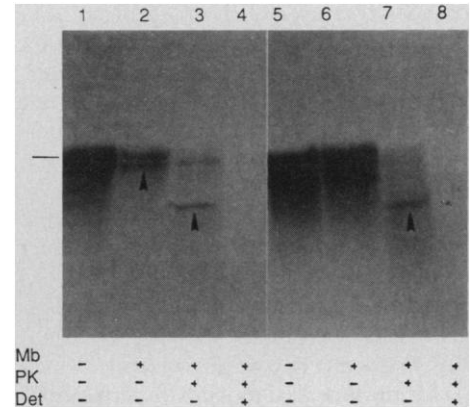
S. B. Prusiner, Departments of Neurology and Biochemistry and Biophysics, University of California, San Francisco, San Francisco, CA 94143.

R. M. Myers, Departments of Physiology and Biochemistry and Biophysics, University of California, San Francisco, San Francisco, CA 94143.

V. R. Lingappa, Departments of Physiology and Medicine, University of California, San Francisco, San Francisco, CA 94143.

The topology of these translocated chains was distinguished by subjecting them to proteolysis with proteinase K. Proteolysis of the transmembrane form generates characteristic protected fragments, one of which is immunoprecipitated by peptide-specific antisera directed to the NH<sub>2</sub>-terminal domain of PrP (18). The NH<sub>2</sub>-terminal fragment predominated during proteolysis and immunoprecipitation of the products of both co- and posttranslational translocation of PrP/HcII in WG (Fig. 2, lanes 3 and 7, arrows). In contrast, full-length PrP/HcII would be protected if stop transfer did not occur. No protected fragments were observed when the membrane bilayer was solubilized with nondenaturing detergent during proteolysis. When PrP synthesized in RRL and translocated either during or after translation was subjected to proteolysis, the predominant protected immunoreactive band was of full size (Fig. 3, lanes 3 and 7). Quantitative densitometry, corrected for methionine distribution, confirmed that both co- or posttranslational translocation generated predominantly the transmembrane topology in WG, while the secretory topology was predominant in RRL. Thus, these system-dependent differences appeared independent of chain elongation. Moreover, the topogenic sequence responsible for this behavior was encoded 5' to the Hinc II site.

**Fig. 2.** Posttranslational translocation of PrP/HcII nascent chains synthesized in WG and analyzed by SDS-polyacrylamide gel electrophoresis (PAGE) and autoradiography, of NH<sub>2</sub>-terminal domain-specific antisera immunoprecipitates, lanes 5 to 8. Co-translational translocation of PrP/HcII, lanes 1 to 4. Template cDNA was prepared as described in the text. Transcription and immunoprecipitation conditions were as described previously (18). Post-translational translocation was performed as follows: translation was carried out for 30 min, then adjusted to 0.1 mM of aurin tricarboxylic acid (ATA) for 15 min followed by addition of emetine to 0.1 mM for 15 min (32). Microsomal membranes (Mb) then added to 2.5 absorbance units (at 260 nm) per milliliter and incubated for 40 min. Simultaneous co-translational translocations were carried out for 1 hour and 40 min. Proteolysis was performed at 4°C for 1 hour with 0.2 mg/ml proteinase K (PK), 10 mM CaCl<sub>2</sub>, 10 mM tris-HCl (pH 8.0), and with or without 1.0% Triton X-100 (Det). PK digestions were terminated by adding phenylmethyl sulfonyl fluoride to 1.0 mM in ethanol and boiling in 1.0% SDS-0.1M tris-HCl (pH 8.9) for 5 min (33). Hatch mark at left denotes the PrP/HcII precursor. Arrows denote major products.



When engineered into the coding region of a heterologous protein, the topogenic sequence should confer the system-dependent behavior observed for PrP onto the resulting chimeras. Figure 4 shows expression in WG and RRL of the chimeric protein encoded in plasmid pSPVSV Gxk in which codons 74 to 114 of PrP (henceforth called R<sub>74-114</sub>) have been engineered into codon 346 of the glycoprotein of vesicular stomatitis virus (VSV G) (Fig. 1B). R<sub>74-114</sub> includes the codons for TM1, as well as the 16 codons preceding the hydrophobic do-

main. VSV G is a transmembrane protein containing an NH<sub>2</sub>-terminal signal sequence. It is largely translocated, but anchored by a well-characterized stop transfer sequence near its COOH-terminal (22, 23). If a topogenic sequence responsible for the difference in PrP topology in WG versus RRL is included within R<sub>74-114</sub>, expression

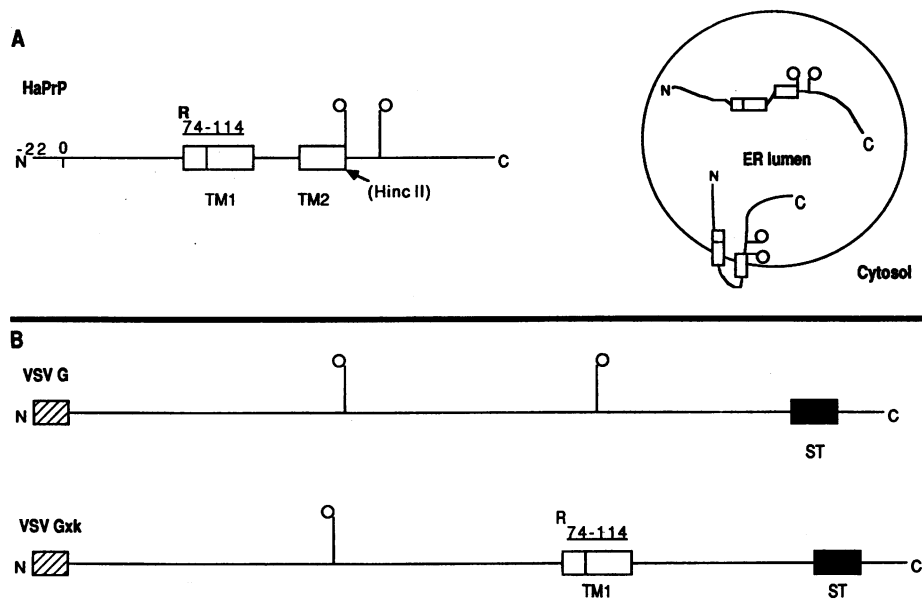


**Fig. 1.** Schematic peptide maps of HaPrP, VSV G, and VSV Gxk (31). The 232 amino acid residues of mature Syrian hamster PrP are shown at top. Residues -22 to 0 represent the cleaved NH<sub>2</sub>-terminal signal sequence. Vertical bars topped by circles indicate potential N-linked glycosylation sites. The open box represents amino acid 74 to 114, with the larger box representing TM1 (24 hydrophobic amino acid residues 90 to 114), which make up the first membrane-spanning region. The smaller box represents an extracytoplasmic hydrophilic domain (28). The stippled box represents TM2 (an amphipathic helix from amino acid 135 to 160), which makes up the second membrane-spanning region. A schematic diagram of the transmembrane and fully translocated forms is depicted at right (18, 19). The 520-amino acid residues of the mature VSV G protein are depicted with potential N-linked glycosylation sites indicated. The cleaved NH<sub>2</sub>-terminal signal sequence is depicted by the striped box. The black box labeled ST represents the native stop transfer sequence from amino acid 474 to 491.

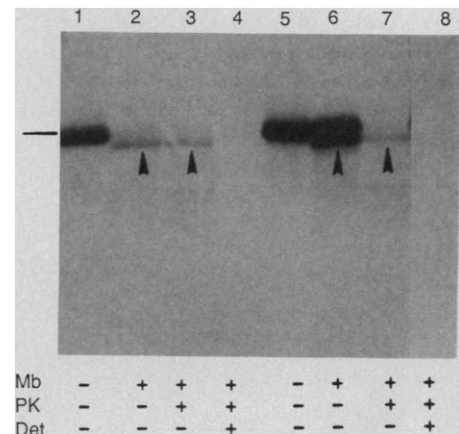


**Fig. 3.** Posttranslational translocation of PrP/HcII nascent chains synthesized in RRL and analyzed by SDS-PAGE and autoradiography of NH<sub>2</sub>-terminal specific antisera immunoprecipitates (lanes 5 to 8). Simultaneous co-translational translocation of PrP/HcII is also shown (lanes 1 to 4). Transcription, co- and posttranslational translocation, and proteolysis were as described in Fig. 2, except performed with RRL (19). The hatch mark denotes the PrP/HcII precursor. Arrows denote major products. Scanning laser densitometry (LKB Ultrosan) was performed on autoradiograms (of both total translation products and immunoprecipitates) to quantify relative proportions of protected fragments generated by proteolysis. Correcting for methionine content, 84 versus 38% of chains achieved a transmembrane orientation at TM1 posttranslationally in WG versus RRL, respectively. This accurately reflects the percentage of transmembrane TM1 domains seen when native PrP is co-translationally translocated in WG and RRL (90 versus 40, respectively).

of VSV Gxk in WG should generate predominantly a transmembrane orientation with TM1 spanning the bilayer. However, in RRL most chains of VSV Gxk should not stop at R<sub>74-114</sub>, and the predominant topology would be expected to be similar to that of native VSV G.

Translation of VSV Gxk in WG in the presence of membranes resulted in a product of higher molecular weight than that observed in the absence of membranes (Fig. 4A). This decrease in mobility on SDS-PAGE was due to core glycosylation, which offsets the increased mobility resulting from cleavage of the NH<sub>2</sub>-terminal signal sequence (24, 25). As predicted, proteolysis revealed this product to be transmembrane at the position of the inserted PrP codons (Fig. 4A, lane 3). The topology of native VSV G is illustrated in lanes 5 to 8 by a similar experiment. Again, a glycosylated product was observed when synthesized in the presence but not the absence of membranes. Proteolysis resulted in a much smaller size shift of the protected product because of the smaller cytoplasmic domain encoded in native VSV G versus VSV Gxk.

When this experiment was performed in RRL, native VSV G displayed the same orientation as in WG (Fig. 4B). Likewise, most chains of VSV Gxk synthesized in RRL displayed a topology similar to that of native VSV G. Thus, in both WG and RRL, the chimeric protein VSV Gxk displayed the topology preference at TM1 observed for

PrP: TM1 was predominantly transmembrane in WG and translocated in RRL. These conclusions were confirmed by quantitative densitometry. Similar chimeras with R<sub>74-114</sub> were generated from two other heterologous proteins, rat lactalbumin (25) and a  $\beta$ -lactamase-chimpanzee globin fusion protein (10). In both cases expression of these chimeras resulted in similar system-dependent predominance of transmembrane (in WG) and secretory (in RRL) phenotypes (21). Expression of VSV Gxk in vivo in *Xenopus* oocytes also resulted in both the transmembrane and completely translocated forms observed in the cell-free systems (21). Taken together with the demonstrated independence from ongoing protein synthesis, these data argue strongly for the presence of a topogenic sequence within R<sub>74-114</sub>.

Typically, stop transfer sequences comprise a hydrophobic domain of approximately 20 to 25 amino acid residues preceded by a charged or polar domain of 10 to 15 residues (1). R<sub>74-114</sub> likewise includes a 16-residue charged and polar region preceding a 24-residue hydrophobic domain (TM1) that is similar to other membrane-spanning regions when analyzed for hydropathy by the methods of Eisenberg (26) or Kyte and Doolittle (18, 27). The function of this topogenic sequence is dependent on features of both the polar and the hydrophobic domains (28).

Unlike other stop transfer sequences, the topogenic sequence defined here terminates

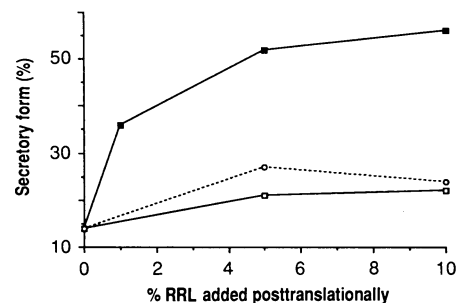


**Fig. 5.** Plot of representative immunoprecipitation SDS-PAGE densitometry data of a post-translational translocation assay with PrP/HcII synthesized in WG and mixed with increasing amounts of RRL before addition of membranes (solid squares), with RRL treated for 10 min at 80°C (open squares), or RRL added after incubation with membranes (dotted line). The y-axis represents percentage of total translocated chains in the secretory form as defined by protease protection. The x-axis represents percentage of added RRL as final reaction volume.

the preponderance of chain translocation across microsomal membranes in WG, but not in RRL. Thus, factors in WG or RRL, independent of protein synthesis, either engage or prevent the action of this unusual topogenic sequence. To establish an assay for these factors, we performed mixing experiments (Fig. 5). Increasing amounts of RRL added to PrP/HcII WG translation products resulted in the saturable generation of the secretory form, upon addition of membranes. If the RRL was added after the membranes or if it was first treated at 80°C for 10 min, the effect on topology was considerably diminished. In the converse experiment, addition of WG to PrP/HcII RRL translation products, and subsequent incubation with membranes, resulted in no change in topology from that observed for RRL translations alone (21). Thus, it appears that a heat-labile factor in RRL is necessary for the efficient generation of the secretory form of PrP.

If R<sub>74-114</sub> is an unusual form of stop transfer sequence subject to regulation at the level of receptor interactions, perhaps conventional stop transfer sequences also act in a receptor-mediated fashion (29, 30). Alternatively, PrP may be a member of a rare class of proteins that use cofactors to promote or inhibit receptor-mediated stop transfer.

It seems likely that the transmembrane and secretory forms represent different folding states of PrP. Indeed, the expression of this single coding region in two different topologic forms may be a consequence of alternate pathways of protein folding. In this case our findings would suggest (i) a novel solution for the paradox of PrP isoforms (each functionally distinct yet identical in sequence and modifications), (ii) an

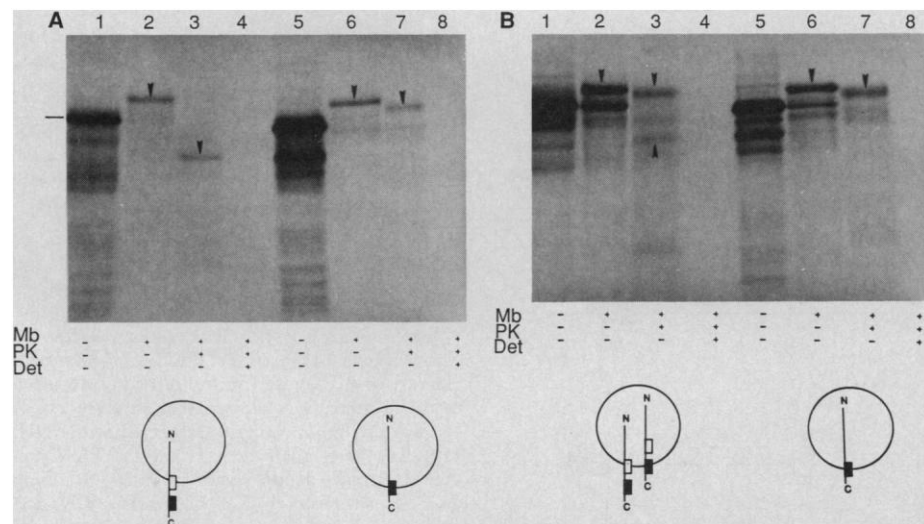


**Fig. 4.** WG (A) and RRL (B) cell-free, transcription-linked, translation-coupled translocation of products encoded by plasmids pSPVSV Gxk (lanes 1 to 4) and pSPVSV G (lanes 5 to 8) as described in Fig. 1, analyzed by SDS-PAGE and autoradiography of total products. Transcription, translation, and proteolysis were as previously described. Schematic representation of VSV Gxk and VSV G topologies are shown at the bottom of the figure. Arrows denote major products. Upward-pointing arrow in (B), lane 3, indicates band co-migrating with that of downward-pointing arrow in (A), lane 3. Hatch mark on left denotes VSV Gxk precursor. All products were confirmed by predicted size, immunoreactivity with polyclonal sera against the Indiana strain of VSV (Lee BioMolecular Research) and reactivity to endoglycosidase H (21). Quantitative densitometry as described in the legend to Fig. 3 reveals 33% of VSV Gxk chains are transmembrane at TM1 in RRL versus 99% in WG.

unusual level of biological regulation with multiple fates and hence multiple functions encoded within a single species of mRNA, and (iii) new variables and caveats to be considered in the prediction of protein structure from primary sequence.

productibly observed. This phenomenon is observed with other proteins translocated after translation (21).

34. We thank J. Rose for the VSV G cDNA and J. Forsayeth and members of the Lingappa lab for useful comments. Special thanks to C. Wilson and

members of the departments of neurosurgery and neurology for help at a critical phase of this work. This work was supported by NIH grants AG02132 and NS14069 to V.R.L., R.M.M., and S.B.P.

13 November 1989; accepted 6 February 1990

#### REFERENCES AND NOTES

1. E. Perara and V. R. Lingappa, in *Protein Transfer and Organelle Biogenesis*, R. C. Das and P. W. Robbins, Eds. (Academic Press, New York, 1988), pp. 3-47.
2. G. Blobel, *Proc. Natl. Acad. Sci. U.S.A.* **77**, 1496 (1980).
3. R. J. Deshaies *et al.*, *Nature* **332**, 800 (1988); W. J. Chirico *et al.*, *ibid.*, p. 805.
4. V. Siegal and P. Walter, *Cell* **52**, 39 (1988).
5. T. Connolly and R. Gilmore, *ibid.* **57**, 599 (1989).
6. M. Weidmann *et al.*, *Nature* **328**, 830 (1987).
7. A. Erickson and G. Blobel, *Methods Enzymol.* **96**, 38 (1983).
8. W. C. Merrick, *ibid.* **101**, 606 (1983).
9. F. N. Katz and H. F. Lodish, *J. Cell Biol.* **80**, 416 (1979).
10. C. S. Yost *et al.*, *Cell* **34**, 759 (1983).
11. R. E. Rothman *et al.*, *J. Biol. Chem.* **264**, 10470 (1988).
12. B. Oesch *et al.*, *Cell* **40**, 735 (1985).
13. M. McKinley *et al.*, *Dev. Biol.* **121**, 105 (1987).
14. S. B. Prusiner, *Annu. Rev. Microbiol.* **43**, 345 (1989); M. Scott *et al.*, *Cell* **59**, 847 (1989).
15. K. Basler *et al.*, *Cell* **46**, 417 (1986).
16. N. Stahl *et al.*, *ibid.* **51**, 229 (1987).
17. N. Stahl *et al.*, *FASEB J.* **2A**, 989 (1988); D. Borchelt *et al.*, *J. Cell Biol.*, in press.
18. B. Hay *et al.*, *Mol. Cell. Biol.* **7**, 914 (1987).
19. B. Hay *et al.*, *Biochemistry* **26**, 8110 (1987).
20. E. Perara, R. E. Rothman, V. R. Lingappa, *Science* **232**, 348 (1986).
21. C. D. Lopez, C. S. Yost, S. B. Prusiner, R. M. Myers, V. R. Lingappa, unpublished data.
22. V. R. Lingappa *et al.*, *J. Biol. Chem.* **253**, 8667 (1978).
23. J. K. Rose and J. E. Bergmann, *Cell* **30**, 753 (1982); G. A. Adams and J. K. Rose, *ibid.* **41**, 1007 (1985).
24. F. N. Katz *et al.*, *Proc. Natl. Acad. Sci. U.S.A.* **74**, 3278 (1977).
25. V. R. Lingappa *et al.*, *ibid.* **75**, 2338 (1978).
26. D. Eisenberg, *Annu. Rev. Biochem.* **53**, 595 (1984).
27. J. Kyte and R. F. Doolittle, *J. Mol. Biol.* **157**, 105 (1982).
28. C. S. Yost *et al.*, *Nature* **343**, 669 (1990).
29. N. K. Mize *et al.*, *Cell* **47**, 711 (1986).
30. E. Scecczyna-Skorupa and B. Kemper, *Proc. Natl. Acad. Sci. U.S.A.* **85**, 738 (1988).
31. The SP6 expression plasmids were constructed as follows. Plasmid pSPHaPrP: PrP cDNA from Syrian hamster isolate was cloned into SP6 (19). Plasmid pSPVSV G: pRSVG was cut with Hind III and Bgl II, gel-purified and ligated with T4 DNA ligase into vector pSP64T (that had been opened with Hind III and Bgl II and treated with calf intestinal phosphatase). Plasmid pSPVSV Gx: a Kpn I site and an Xba I site were introduced via site-directed mutagenesis at codons 72 and 114, respectively, or pSPHaPrP. The resultant plasmid was opened at the Xba I site, blunted with the Klenow fragment, and ligated to a Kpn I 8-base fragment with T4 DNA ligase. The plasmid was then cut with Kpn I, and the 126-bp fragment was gel-purified and religated into pSPVSV G vector opened at codon 346 with Kpn I to create an in-frame fusion.
32. To ensure translation was completely blocked, a mock control was done in parallel without transcript during the initial 30-min translation. The sample was then split and one portion was treated with ATA and emetine and the other with H<sub>2</sub>O and compensating salts. Transcript was then added and reactions were allowed to incubate the remaining 40 min. The sample that was treated with protein synthesis inhibitors did not synthesize product, whereas the sample that received mock inhibitors did (21).
33. A decrease in the number of chains after proteolysis of posttranslational translocation reaction was re-

## Reorganization of Retinotopic Cortical Maps in Adult Mammals After Lesions of the Retina

JON H. KAAS,\* LEAH A. KRUBITZER, YUZO M. CHINO, ANDY L. LANGSTON, EDWARD H. POLLEY, NORMAN BLAIR

The organization of the visual cortex has been considered to be highly stable in adult mammals. However, 5° to 10° lesions of the retina in the contralateral eye markedly altered the systematic representations of the retina in primary and secondary visual cortex when matched inputs from the ipsilateral eye were also removed. Cortical neurons that normally have receptive fields in the lesioned region of the retina acquired new receptive fields in portions of the retina surrounding the lesions. The capacity for such changes may be important for normal adjustments of sensory systems to environmental contingencies and for recoveries from brain damage.

ARE THE MAPS OF VISUAL SPACE IN visual cortex capable of reorganization in adult mammals? As in other mammals, the visual cortex of cats contains several retinotopic representations of the visual field, including those in areas 17 and 18 (1). Such systematic representations of peripheral receptor arrays also characterize somatosensory and auditory cortex (2). Under normal circumstances, these sensory maps develop in a highly consistent manner in individuals of the same species. However, development of these topological maps can be altered by abnormal sensory inputs, including those produced by sensory deprivation and damage to the peripheral sensory sheet (3, 4). Thus, the nature of the input from the receptor sheet partly determines the ultimate organization of developing sensory maps. In the visual system, sensory manipulations such as monocular deprivation, induced strabismus, and unilateral defocusing of the image can alter cortical organization (3). However, these manipulations affect cortical organization mainly or only within a critical developmental period extending a few months postnatally in cats or several years in humans (3). Thus, evidence supports the view that the organization of visual cortex remains highly stable after initial development, and there has been

little reason to suppose that basic features of retinotopic maps can change in adults.

In contrast to the visual system, recent experiments on somatosensory cortex indicate that the organization of sensory maps can be modified even in adults (4, 5). For example, if part of the normal representation of the hand in primary somatosensory cortex is deprived of its normal source of activation by cutting a peripheral nerve, the cortical representation reorganizes over a period of hours to weeks so that neurons in the deprived zone of cortex acquire new receptive fields on other parts of the hand. Such adult plasticity implies that previously existing connections in the brain are capable of changing in synaptic effectiveness so that new receptive fields and new representational organizations can emerge in cortex. Such changes could be important in normal adjustments of the brain to alterations in the sensory environment, as well as in compensations for peripheral and central damage to the nervous system. Because the potential for such reorganization would seem to exist in other sensory fields, we investigated the possibility of adult plasticity in visual cortex with an experimental approach that has been used successfully for the somatosensory system.

Parts of areas 17 and 18 of the visual cortex were deprived of a normal source of activation by placing lesions 5° to 10° in diameter just above the area centralis in the retina of one eye of adult cats (6). By itself this procedure produced no notable change in retinotopic organization when tested in one cat. Most cortical neurons are binocularly activated and thus have two retinotopi-

J. H. Kaas and L. A. Krubitzer, Department of Psychology, Vanderbilt University, Nashville, TN 37240.  
Y. M. Chino and A. L. Langston, College of Optometry, University of Houston, Houston, TX 77204.  
E. H. Polley and N. Blair, Departments of Anatomy and Ophthalmology, University of Illinois Medical Center, Chicago, IL 60680.

\*To whom correspondence should be addressed.